ADVANCED HEALTHCARE MATERIALS
www.advhealthmat.de

Materials Views
www.MaterialsViews.com

Graphene-Based Electroresponsive Scaffolds as Polymeric Implants for On-Demand Drug Delivery

Ania Servant, Veronica Leon, Dhifaf Jasim, Laura Methven, Patricia Limousin, Ester Vazquez Fernandez-Pacheco, Maurizio Prato,* and Kostas Kostarelos**

Stimuli-responsive biomaterials have attracted significant attention in the field of polymeric implants designed as active scaffolds for on-demand drug delivery. Conventional porous scaffolds suffer from drawbacks such as molecular diffusion and material degradation, allowing in most cases only a zero-order drug release profile. The possibility of using external stimulation to trigger drug release is particularly enticing. In this paper, the fabrication of previously unreported graphene hydrogel hybrid electro-active scaffolds capable of controlled small molecule release is presented. Pristine ball-milled graphene sheets are incorporated into a three dimensional macroporous hydrogel matrix to obtain hybrid gels with enhanced mechanical, electrical, and thermal properties. These electroactive scaffolds demonstrate controlled drug release in a pulsatile fashion upon the ON/OFF application of low electrical voltages, at low graphene concentrations (0.2 mg mL^{-1}) and by maintaining their structural integrity. Moreover, the in vivo performance of these electroactive scaffolds to release drug molecules without any "resistive heating" is demonstrated. In this study, an illustration of how the heat dissipating properties of graphene can provide significant and previously unreported advantages in the design of electroresponsive hydrogels, able to maintain optimal functionality by overcoming adverse effects due to unwanted heating, is offered.

1. Introduction

The field of polymeric implants for drug delivery purposes has witnessed significant progress and an exponential growth in the development of innovative and efficient systems capable of minimizing possible adverse reactions from systemic (oral, intravenous) administration.[1–3] While a vast variety of polymeric platforms, from polymer nanocomposites to injectable hydrogels, are described in the literature, only very few are capable of pulsatile drug release.[4–6] Great effort has been recently invested in the development of such sophisticated devices that would be able to deliver drug molecules according to patients' needs. Among them, field-based stimuli-responsive hydrogels combined with nanomaterial additives are some of the most promising.[7–9] Gold, iron oxide, and silver nanoparticles have been employed to increase the sensitivity and response to external stimulus of hydrogels with the ultimate goal of achieving drug release profiles with precise control of the released dose and reproducibility between application of each cycle of external stimulus.[10,11]

The use of an electrical field as external stimulus offers the possibility to control drug release levels according to strength, duration, and frequency of the field applied. Previous studies have reported electro-responsive hydrogel-based systems with pulsatile drug release profiles in vitro and in vivo.[12–16] Our group previously reported a hydrogel system containing pristine multiwalled carbon nanotubes (pMWNTs). The use of pMWNT improved the methacrylic-acid-based hydrogel responsiveness to the electrical field. That system also showed encouraging results in

Dr. A. Servant, D. Jasim, Dr. L. Methven, Prof. K. Kostarelos
Nanomedicine Lab
Faculty of Life Sciences
University College London
London WC1N 1AX, UK
E-mail: kostas.kostarelos@manchester.ac.uk
Dr. A. Servant, D. Jasim, Dr. L. Methven, Prof. K. Kostarelos
Faculty of Medical & Human Sciences and
National Graphene Institute
University of Manchester
M19 9PT, UK
Dr. V. Leon, Dr. E. Vazquez Fernandez-Pacheco
Facultad de Ciencias Químicas
Universidad Castilla La-Mancha
Ciudad Real 13071, Spain
E-mail: ester.vazquez@uclm.es
Dr. V. Leon, Prof. M. Prato
Dipartimento Scienze Chimiche e Farmaceutiche
University of Trieste
Piazzale Europa 1, Trieste 34127, Italy
E-mail: prato@units.it
Dr. P. Limousin
UCL Institute of Neurology
University College London
Queen Square, London WC1N 1AX, UK

DOI: 10.1002/adhm.201400016

achieving pulsatile drug release profiles in vivo, detectable in mouse blood following subcutaneous implantation and ON/OFF application of a DC field.[17] However, that "on-demand" delivery system displayed drawbacks such as structural damage of the matrix after each ON/OFF cycle of electrical stimulation and a sharp temperature increase of the device upon field exposure. This temperature increase also known as "resistive heating" could be explained by the properties of the hydrogel polymeric matrix that displays relatively high impedance.

Graphene, defined as a single-atom thick layer of carbon structured in a honeycomb lattice, has attracted tremendous attention in many areas ranging from electronics to energy storage since its isolation from graphite in 2004.[18] Graphene displays many unique features such as high electron mobility, thermal conductivity comparable to that of metals, optical absorption, and mechanical strength.[19] In the biomedical field, graphene oxide (GO) the "hydrophilic" derivative of graphene, has also generated great interest and is currently investigated for many applications such as biosensors[20–23] and drug delivery.[24,25] In addition, GO has been employed in the preparation of responsive polymer implants for tissue engineering.[26–32] However, covalent functionalization of graphene to GO or reduced graphene oxide (rGO) leads to significant loss of its attractive electrical properties due to conversion of the planar sp^2 lattice into a sp^3 lattice resulting in drastic reduction of electron mobility.[33]

Utilization of the thermal conductivity and mechanical properties of graphene as an additive to enhance the capabilities of responsive biomaterials has been underexploited.[34] In this study, we report the development of an electro-responsive polymer hydrogel device containing well-dispersed graphene sheets for in vivo pulsatile drug release. To our knowledge, no other polymer hybrid system has been designed to exploit the electrical, thermal, and mechanical properties of pristine graphene in this manner.

2. Results and Discussion

Graphene suspensions in water were obtained by exfoliating graphite through its molecular interactions with melamine using ball milling as previously described. This technique allows the production of concentrated graphene dispersions in organic solvent or water (**Figure 1**).[35] The preparation of ball-milled graphene (GBM) hydrogel hybrids at different graphene concentrations was carried out by in situ radical polymerization and addition of all the monomers (methacrylic acid (MAA) and *N,N′*-methylene bisacrylamide (BIS)) and initiator (potassium persulfate PSS) into the aqueous graphene dispersion (Figure 1). Previously reported systems based on conductive hydrogels[36] or on the incorporation of conductive nanomaterials such as pMWNTs into hydrogel matrices demonstrated encouraging results in their ability to deliver drugs in a pulsatile manner in vivo.[15–17] Such hydrogel hybrids were prepared under the same conditions as the present graphene-containing systems and were studied throughout for comparison.

The size distribution of the graphene sheets was determined using Image J software analysis (**Figure 2**A) in the range between 100 nm and 1 µm, the majority between 100 and 500 nm. Atomic force microscopy (AFM) confirmed the presence of few graphene layers with thickness between 2 and 6 nm mostly single graphene layers with a thickness below 2 nm (Figure 2B). The Raman spectrum of GBM is shown in Figure 2C. The spectrum displayed two bands at 1360 and 1560 cm^{-1} characteristic of the D and G band, respectively, typical of carbon films dominated by sp^2 sites. Graphite (Raman shown in Figure S1, Supporting Information) and graphene spectra also exhibited a 2D peak at 2650 cm^{-1}, described as the second order of the D peak at 1360 cm^{-1}. The 2D band in graphene is quite different from bulk graphite. Several studies reported investigations on the number of graphene layers by resolving the 2D band in the Raman spectrum of the material. This 2D band is found to be shifted and can be deconvoluted into four bands (Lorentzian peaks) when the number of graphene layers increases from 1 to 3.[37–39] For graphite, the 2D band is significantly shifted compared to that of graphene, detected as a perceptible shoulder. In this study, the 2D band indicated that GBM was mainly constituted of two to three layer graphene sheets.

The dry hybrid gels displayed homogeneous morphology at the macroscopic level after the polymerization process suggesting that the graphene sheets were well dispersed into the polymeric matrix (Figure S2A, Supporting Information). Surface characterization on the swollen graphene hybrid gels using scanning electron microscope (SEM) confirmed a porous structure, typical of that of macro-porous hydrogels with a pore size of around 500 nm (Figure S2A, Supporting Informaton). The pore size of hydrogels is an important parameter as it determines the kinetics of swelling/deswelling that is crucial for the responsiveness to the electric field. The swelling/deswelling rate of a hydrogel matrix is known to increase as a function of pore size, with macro and super-porous gels (pore size above 10 µm) are able to reach complete swelling within minutes.[40,41] In addition, macro-porous hydrogels display good mechanical properties that are similar to soft tissues.[42] Swelling properties of the hybrid gels were studied by immersing the gels in HEPES buffer at pH 7.4. Complete swelling was reached after 3 d of immersion (Figure S2B, Supporting Information) and the final swelling degree $D_{s,F}$ was found to be 30 for all of the graphene hybrid gels, while it was only of 25 for the blank gel at the same duration of immersion. At same content of cross-linker, the graphene hydrogel hybrids reached higher swelling degree than the pMWNT hydrogel hybrids over the same period of time (**Figure 3**A). This suggests that the incorporation of graphene allowed the gel matrix to expand further without inducing any structural damage and incorporate more fluid into its reservoir-based matrix. This could be explained by a better dispersion of graphene within the polymer matrix in contrast to the carbon nanotubes that aggregated during the polymerization process reducing the mechanical capabilities of the gels.[43] In addition, graphene is known to display excellent mechanical properties in particular strength and has been used in polymer composites as a reinforcing additive for a variety of applications.[44] This enhanced degree of swelling suggested that the GBM hydrogel hybrids possessed higher mechanical capabilities in terms of flexibility than the pMWNT hybrid gels.

Methacrylic-acid-based hydrogel hybrids were also prepared using GO instead of ball-milled graphene using in situ

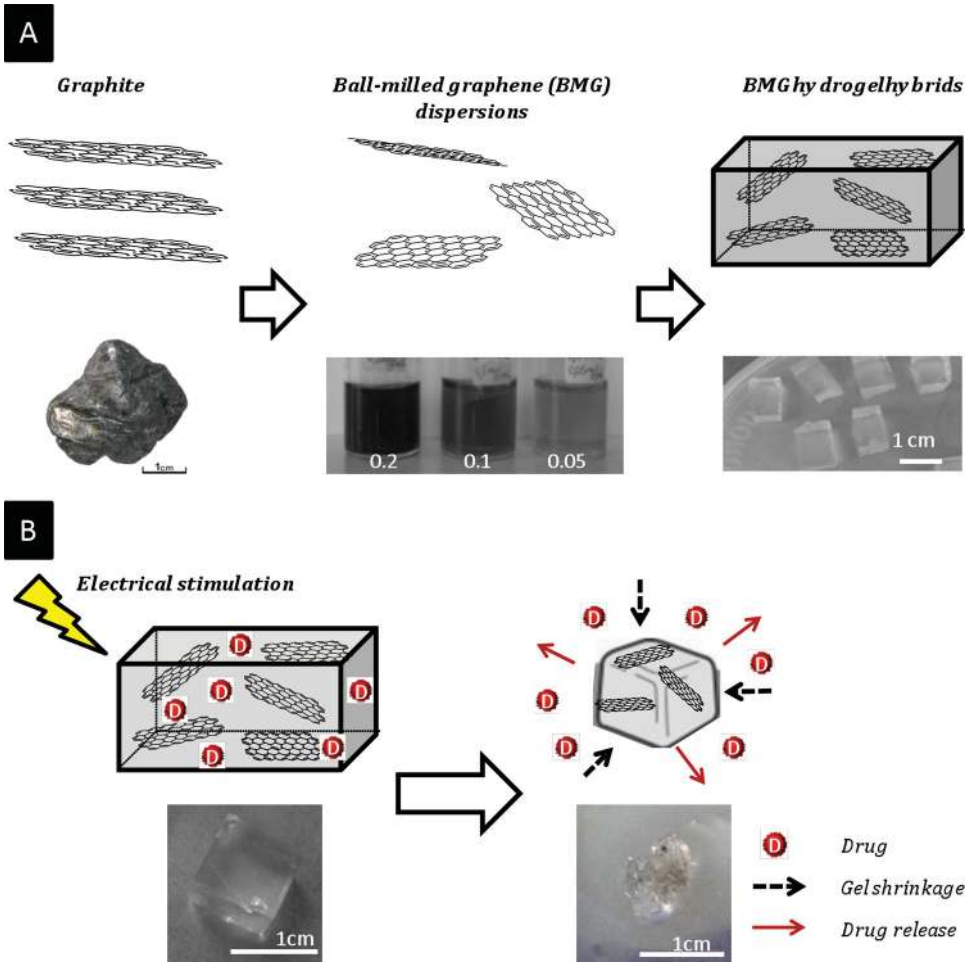

Figure 1. Electro-responsive graphene/PMAA hydrogel hybrids for "on-demand" drug delivery. A)In situ polymerization of an aqueous dispersion of graphene i) the aqueous solutions of graphene at different concentrations were obtained by exfoliation of graphite through interaction with melamine by ball milling; ii) the graphene hydrogel hybrids were then prepared by in situ free radical polymerization in presence of methacrylic acid (MAA) and *N,N'*-methlyenebisacrylamide (BIS) as monomer and cross-linker, respectively. Scale bar: 1 cm. B) Pulsaltile drug release upon ON/OFF application of a DC electric field. The hybrid gel, loaded with a drug, releases its cargo in a pulsatile manner upon the ON/OFF application of a DC electric field through reversible de-swelling of the gel matrix illustrated with images of GBM hydrogel hybrids before and after electrical stimulation. Scale bars = 1 cm.

radical polymerization under the same conditions. GO has demonstrated enormous potential in many biomedical applications[45] and aqueous dispersions of GO remain stable for long periods of time. However, the presence of numerous defects on the graphitic structure after oxidation is thought to decrease significantly the electrical properties of material.[33] It was nevertheless interesting to compare the electrical sensitivity of the methacrylic-acid–based hydrogel matrix in the presence of both graphene types. GO solutions were obtained from graphite using the modified Hummers method according to published procedures.[46] Monomers (MAA and BIS) and initiator (PPS) were added to the stable aqueous GO solution. The stability of the mixture was monitored over time (Figure S3A, Supporting Information). The mixture was not stable and separated into two phases after 30 min due to possible interactions between the oxidation groups present on GO sheets and the MAA monomers. We went ahead with initiation of the polymerization processes and GO aggregates were seen in the resulting gels (Figure S3B, Supporting Information). It was therefore concluded that GO hybrid gels could not be obtained following the procedure used for the preparation of the ball milled graphene hybrid gels.

Hybrid gel response to a DC electric field (10 V) was then studied by monitoring water loss from the gel matrix as a result of gel de-swelling as in Figure 3B. For anionic polyelectrolytes such as PMAA-based hydrogels, an anisotropic deformation of the gel characterized by a contraction at the cathode and a swelling at the anode is typically observed upon electrical stimulation when the gel is placed in contact with two carbon electrodes. This chemomechanical behavior is the outcome of different electrochemical phenomena such as electro-osmosis of water and migration of charged ions in the direction of the anode.

Deswelling of the graphene hybrid gels was compared to that of pMWNT hybrid gels prepared at the same pMWNT concentrations. In both cases, there was an improvement in the release performance of the gels as the concentration of pMWNT and GBM increased from 0 to 0.2 mg mL^{-1}. The GBM

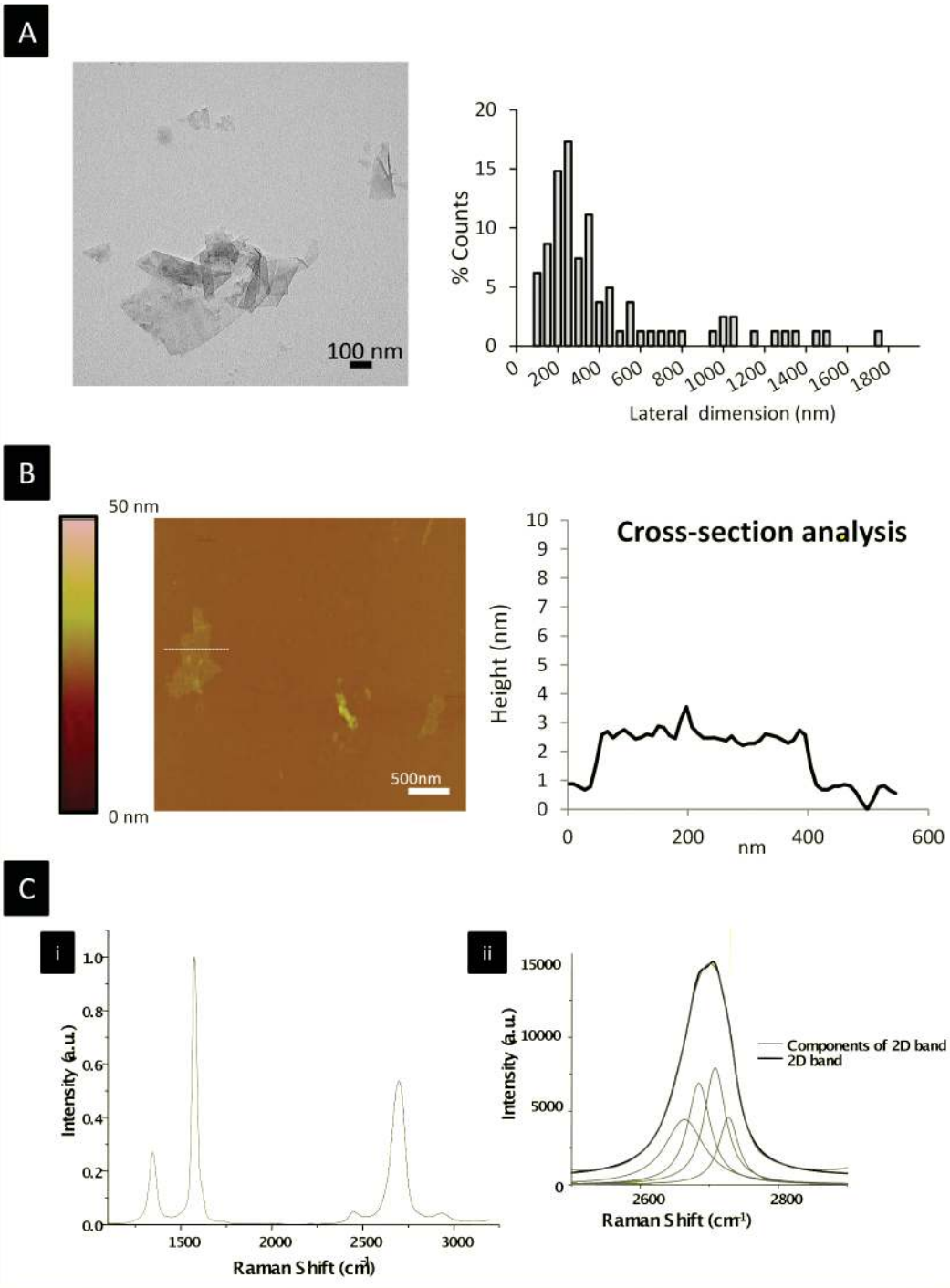

Figure 2. Characterization of graphene obtained by ball-milling (GBM). A) Transmission electron microscope (TEM) images of GBM at 0.1 mg mL^{-1} in water. The size distribution was derived from TEM images after counting the lateral dimension of 100 individual graphene sheets using imageJ software. B) Atomic force microscopy (AFM: tapping mode) of graphene captured in air by depositing 20 µL of the graphene dispersion on a freshly cleaved mica surface. C) i) Raman spectra of ball-milled graphene. ii) The 2D peak at around 2650 cm^{-1} can be decomposed into four bands (Lorentzians peaks), characteristic feature of the Raman spectrum of few-layer graphene.

hybrid gels outperformed those containing pMWNT hybrid gels in terms of deswelling and water release. In particular, for the gel at the highest graphene concentration (0.2 mg mL^{-1}), a 20%–25% water release enhancement was obtained compared to its pMWNT counterpart. The incorporation of GBM into the methacrylic-acid-based hydrogel matrix resulted in gels with higher mechanical capabilities in terms of swelling/deswelling than their pMWNT counterparts. The electrical properties of the gels were also enhanced by the incorporation of graphene sheets, with bulk resistivity decreasing from 350 to

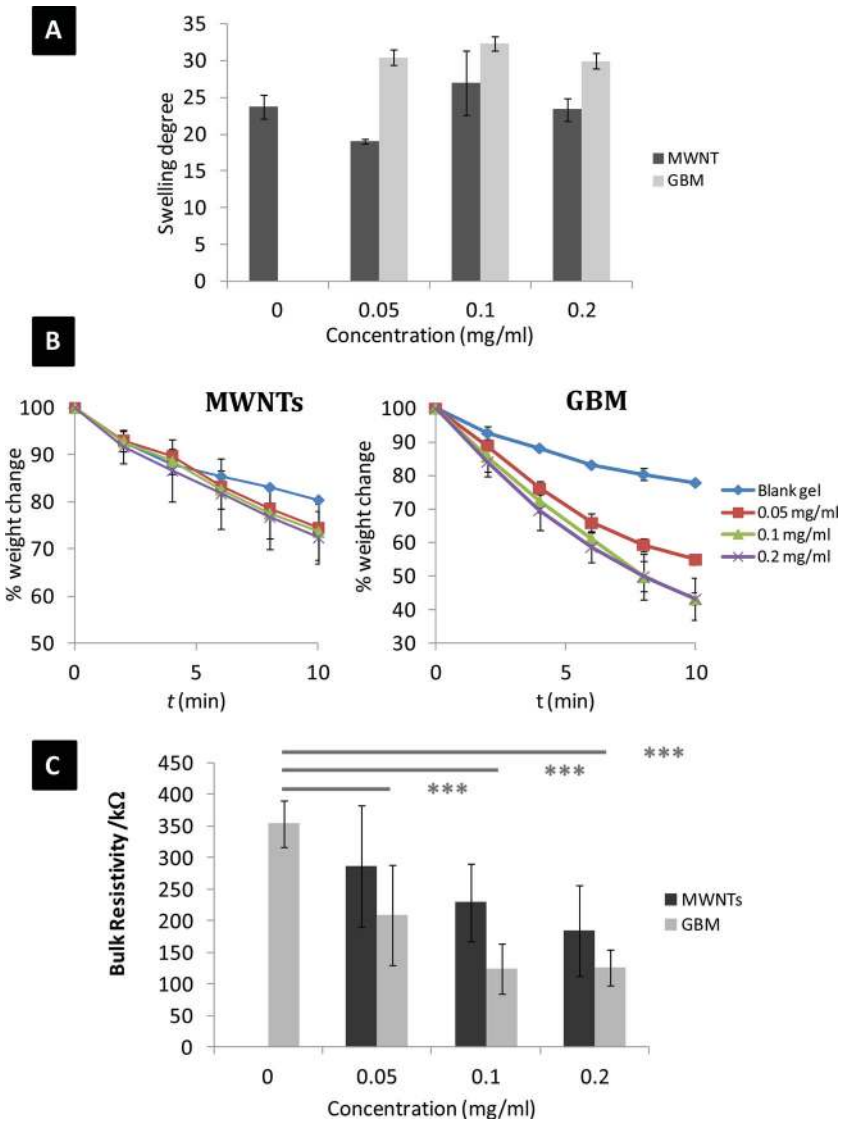

Figure 3. Mechanical and electrical properties of graphene/PMAA hydrogel hybrids. A) Graphene and pMWNT hydrogel hybrid swelling in a HEPES buffer solution at pH 7.4. The graphene hydrogel hybrids displayed higher final swelling degree $D_{F,s}$ than their pMWNT counterparts at equivalent pMWNT concentrations and blank gel. B) Gel de-swelling upon the application of a DC electric field. Graphene and pMWNT hydrogel hybrids de-swelling upon the application of a DC electric (10 V). Water release upon the gel de-swelling was monitored over time for all of the gels at different graphene and MWNT concentrations (0. 05, 0.1, and 0.2 mg mL^{-1}). C) Bulk resistivity of the graphene and MWNT hybrid gels. Bulk resistivity was determined as a result of the product between the thickness of the sample and the sheet resistance R_s. The sheet resistance R_s was measured five times with a two probe multimeter ($p < 0.005$).

100 kΩ from 0.1 mg mL^{-1} GBM concentration (Figure 3C). GBM hybrids gels showed significantly lower bulk resistivity than their pMWNT counterparts suggesting that lower voltage could be used with the graphene gels to obtain efficient drug release.

The ability of a selected graphene hybrid gel (0.2 mg mL^{-1}) to release controllable drug doses repeatedly upon ON/OFF application of an electrical field was investigated and compared to a pMWNT hydrogel hybrid at the same nanotube concentration (0.2 mg mL^{-1}) and blank gel. Radiolabeled (^{14}C)-sucrose was used as a model small hydrophilic molecule and was loaded into the matrix during swelling. All of the gels were immersed in a concentrated solution of ^{14}C-sucrose in HEPES buffer (pH 7.3, 25 × 10^{-3} M) until they reached complete swelling and the quantity of loaded ^{14}C-sucrose was subsequently determined by their weight increase (Table 1, Supporting Information).

A DC electric field of 10 V was applied for short time intervals (5 min) and then turned off for 1 h. **Figure 4**A shows the pulsatile ^{14}C-sucrose release profile from the different gel systems upon the ON/OFF application of the electric field. All of the gels demonstrated step-up release profiles, significant increases in drug release as the electric field was applied and significant decreases in drug release upon removal of the field. The GBM hybrid gel significantly outperformed the pMWNT hybrid and blank gels, with a two- and threefold ^{14}C-sucrose release enhancement after the first electrical stimulation. The GBM gels demonstrated greater in vitro release after the second and third electrical stimulations leading to a total of 80% of initial ^{14}C-sucrose dose released. The pMWNT hybrid and blank gels reached only 40% and 30% of the initial ^{14}C-sucrose dose released in total.

The structural deformation of the gel matrix damage was also investigated here by applying a DC electric field of 10 V for a period of 10 min to the graphene and nanotube hybrid gels at high concentrations (0.2 mg mL^{-1}). The gels before and after electrical stimulation are shown in Figure S4 (Supporting Information). The nanotube hybrid gel demonstrated significant structural damage and ruptured in two pieces after stimulation while the graphene hydrogel shrunk extensively but much more homogeneously, remaining as an intact gel block. Therefore, the burst release obtained after initial stimulation was not the result of structural destruction of the GBM gel matrix, but rather due to a higher electro-responsiveness of the gel to the electric field. In order to further optimize and achieve more reproducible release by ON/OFF stimulation cycles, ^{14}C-sucrose release from graphene hybrid gels at different GBM contents (0.05, 0.1, and 0.2 mg mL^{-1}) was studied (**Figure 5**A). The gel with the lowest GBM concentration (0.05 mg mL^{-1}) showed more reproducible cycles although the total amount of ^{14}C-sucrose released was reduced to 65% of initial dose, compared to that of the hybrid gels at higher graphene contents (70% and 80% of initial dose at 0.1 and 0.2 mg mL^{-1}, respectively). This could however be overcome by increasing the number of cycles of electrical stimulations.

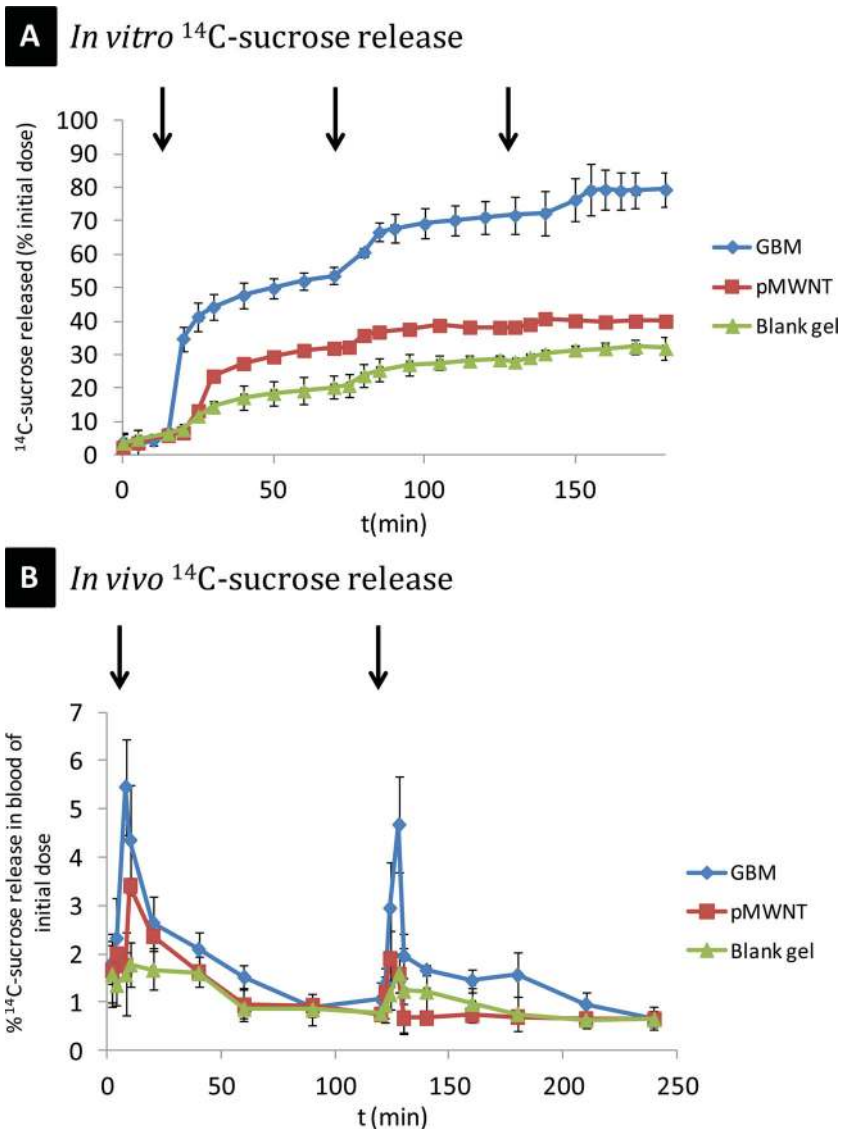

Figure 4. Drug release from graphene/PMAA hydrogel hybrids upon the ON/OFF application of a DC electric field. A) In vitro pulsatile drug release upon the ON/OFF application of an electrical voltage. ^{14}C-sucrose was selected as model hydrophilic drug. The gels were loaded with radio-labeled sucrose (6 μCi) dissolved in 6 mL of HEPES buffer at pH 7.3 during gel swelling. Drug release was monitored over time while applying ON for 5 min and OFF the electric field at 60 min exposure interval. The pulsatile release of ^{14}C-sucrose was determined for the blank gel and a selected MWNT hybrid gel (0.2 mg mL^{-1} of MWNTs) for comparison. B) In vivo pulsatile drug release upon the ON/OFF application of an electrical voltage. Release profile of ^{14}C-sucrose from the graphene and MWNT hybrid gels at 0.2 mg mL^{-1} of graphene and MWNT, respectively, and blank gel in the blood plasma of CD1 mice upon electric stimulation. The gels were electrically stimulated twice with a voltage of 10 V for 1 min at 2 h interval. The first electric stimulation was performed after 2 h of gel incubation in the back of the neck of the mice when the ^{14}C-sucrose release from the gels of sucrose was found to be low and stable.

The incorporation of graphene allowed the gel matrix to reach higher degree of swelling and subsequently to deswell more efficiently than with carbon nanotube losing up to 80% of its fluid content after 10 min of electrical stimulation without major gel damage. This is shown by the reproducibility in drug release after two cycles of ON/OFF electric field application. This confirmed the higher mechanical capabilities of the graphene hydrogel hybrids compared to the pMWNT hydrogel hybrids.

The ability of the GBM hydrogel hybrids to release drug molecules of different hydrophobic character was then evaluated. Radiolabeled ^{14}C-doxorubicin (^{14}C-DOX) was used as a model amphiphilic drug and loaded into the gel matrix by swelling. The GBM hybrid gel at high graphene content (0.2 mg mL^{-1}) was immersed in a concentrated solution of ^{14}C-DOX in HEPES buffer (pH 7.3, 25×10^{-3} M) until complete swelling was reached. The quantity of loaded ^{14}C-DOX was subsequently determined by the gel weight difference and by monitoring the ^{14}C-DOX concentration in the medium over time to evaluate the quantity of DOX incorporated into the gel matrix (Table S1, Supporting Information). A pulsatile release profile was observed for DOX release after three cycles of ON/OFF electrical stimulation suggesting that this hydrogel system could also be applied to amphiphilic drugs (Figure S5B, Supporting Information). However, the total amount of ^{14}C-DOX released reached only 30% of initial dose. This can be explained by potential interactions between DOX and the polymer matrix or the graphene sheets (e.g., π–π stacking) that prevent DOX molecules to release as the matrix responded by deswelling. However more work needs to be performed to better detect such interactions with different molecules and optimize the required release profile.

The ability of GBM hydrogel hybrids at 0.2 mg mL^{-1} to release small drug molecules in vivo was studied next.[17] The gel was designed at high GBM concentration (0.2 mg mL^{-1}) to ensure optimal ^{14}C-sucrose (model drug molecule) detection. Electrical stimulation was initiated after an equilibration period, during which the gel was allowed to adapt to the biological environment for 2 h after implantation. The gel was loaded with ^{14}C-sucrose by swelling and subcutaneously implanted in the upper dorsal region of CD-1 mice and electrically stimulated for 1 min at 10 V at 2-h intervals. Release drug concentration (^{14}C-sucrose) was monitored by the detection of radiation in the systemic circulation of the animals using tail vein bleeding. The performance of the GBM hybrid gel was compared to that of pMWNT hybrid gel at the 0.2 mg mL^{-1} pMWNT content and to that of a blank gel. A pulsatile release profile was obtained for all of the gels, with a significant increase in the released sucrose concentration observed upon application of the electrical field for 1 min, reaching a peak at 8–10 min post-stimulation. Progressive decrease upon removal of the electrical field

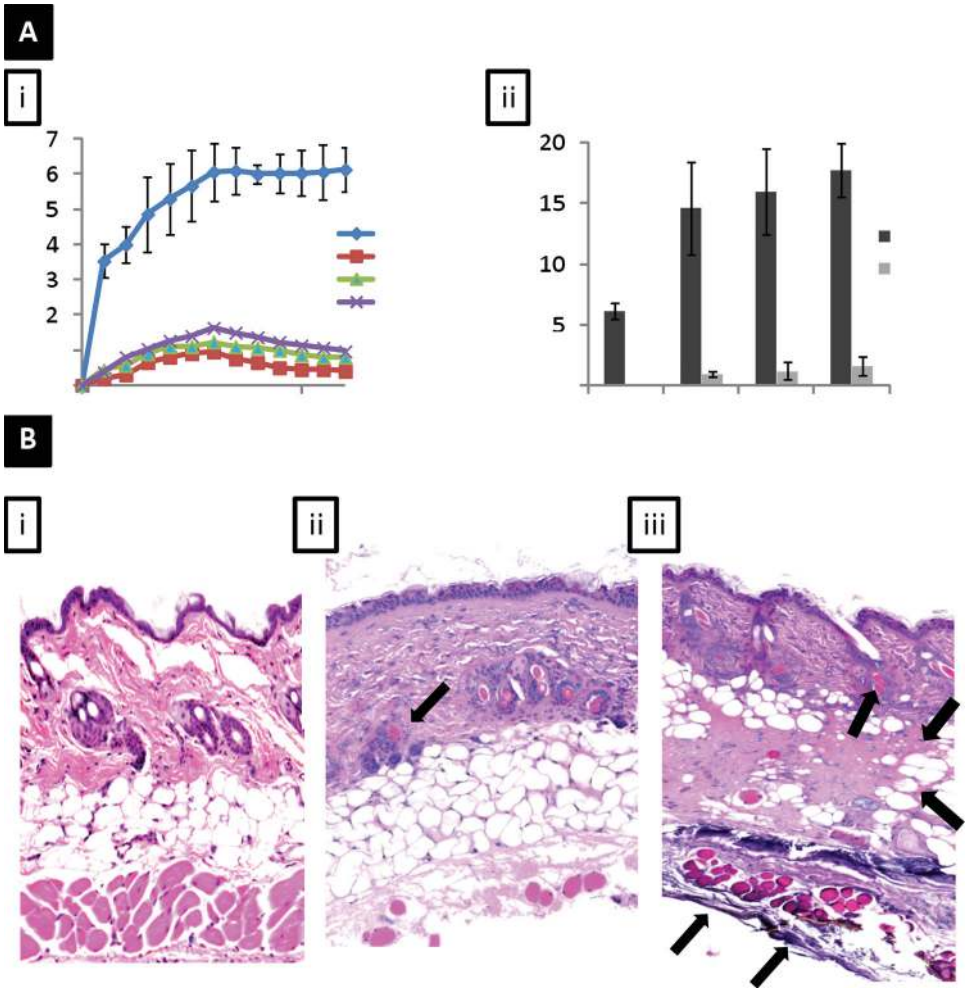

Figure 5. In vitro and in vivo thermal conductivity of graphene/PMAA hydrogel hybrids. A) Heating properties of the gel hybrids. i) Temperature profile over time of graphene hybrid gels prepared at different graphene concentrations (0.05 (squares), 0.1 (triangles), and 0.2 (crosses) mg mL^{-1}) and blank gel (diamonds) exposed to an electric voltage of 10 V. ii) Final temperature of graphene and MWNT hybrid and blank gels after 5 min of exposure to the electric field (10 V). B) Histological analysis of mouse (CD-1) skin samples. Temperature effect of a selected graphene hybrid gels (0.2 mg mL^{-1}) and MWNT hybrid gels (0.2 mg mL^{-1}) upon the application of the electric field after subcutaneous implantation; the subcutaneously implanted gels ii) 0.2 mg mL^{-1}, iii) 0.2 mg mL^{-1} MWNTs) were stimulated for up to 5 min with a DC electric field (10 V) and compared with naive skin (i). Tissue damage was then analyzed by histology and compared with the skin of an untreated mice. Images are of hematoxylin and eosin-stained sections (×10 objective) and are representative from a minimum of two mice per group.

to reach the baseline level at around 1 h post-stimulation was observed (Figure 4B). The baseline was determined by monitoring ^{14}C-sucrose release in the blood compartment from an implanted gel without any electrical stimulation. The graphene hybrid gels significantly outperformed all others. ^{14}C-sucrose release in blood after each stimulation reached 5.5% of the ^{14}C-sucrose initial dose in blood 8 min after the first electrical stimulation, while only 3.5% and 2% was achieved for the pMWNT hybrid and blank gel, respectively. Moreover, the performance of ^{14}C-sucrose release between cycles of ON/OFF electrical stimulation was more consistent with the graphene hybrid gels (5.5% of initial dose after the first stimulation and 5% after the second stimulation). The quantity of ^{14}C-sucrose released in blood from the pMWNT hybrid and blank gels was significantly reduced after the second stimulation (2% and 1.5% of initial dose respectively).

One of the other major drawbacks of electro-responsive drug delivery systems is their potential temperature increase upon exposure to the electric field known as resistive heating. In our previous studies using nanotube hydrogel hybrids, we reported a temperature increase in the overall gel volume up to 15 °C upon exposure to a DC electric field of 10 V for about 2 min for a 1 cm^3 hybrid gel (0.2 mg mL^{-1} pMWNT content).[47] Temperatures above 41–42 °C during electrical stimulation can be very harmful and induce tissue necrosis. It was demonstrated recently that graphene, an excellent heat conductor, can allow fabrication of a heat "sink" and can boost the lifetime of devices by a factor of 10.[48]

Graphene hybrid gels at different graphene contents (0.05, 0.1, and 0.2 mg mL^{-1}) were exposed to a low DC electric field and the temperature of the gels was monitored over time (Figure 5A-i). The maximum temperature obtained for the gels

during electrical stimulation was then compared to that of the pMWNT hybrid gels (Figure 5A-ii). The temperature increase from the GBM gels was 10-fold lower than that of pMWNT hybrid gels. While the pMWNT hybrid gels displayed a temperature rise between 15 and 20 °C, their graphene counterparts demonstrated temperature increase up to 2 °C. The incorporation of graphene sheets into the methacrylic-acid-based hydrogel had significantly decreased the resistive heat generated from the hydrogel matrix presumably due to their effective heat dissipation capabilities. The damage to the skin and tissue due to the potential resistive heating from subcutaneous implantation of the gels was studied by histology using hematoxylin and eiosin (H&E) staining. Gels (graphene and pMWNT hybrid gel at 0.2 mg mL^{-1}) were implanted subcutaneously and stimulated with a DC electric field of 10 V for 5 min. The skin around the implantation site was removed and compared to the skin of an untreated mouse (Figure 5B). The skin tissue to which the pMWNT hybrid gel was implanted (Figure 5B-iii) showed signs of acute inflammation and tissue necrosis especially in areas of contact with the gel. In the case of the GBM hydrogel hybrids (Figure 5B-ii), there was significantly less damage to the skin or tissue below the area where the gel was implanted.

In order to further assess the gel biocompatibility, human neural cells (SHSY5Y) were deposited on gel films (GBM hybrid gels at different graphene content and blank gel) and the cell viability was determined after 96 h of exposure to gels (Figure S6A, Supporting Information). These studies were crucial as previous tudies reported the cyto- and genotoxicity (size- and concentration-dependent) of these nanomaterials.[49–53] There were no signs of toxicity as cell growth was unperturbed by the presence of the gels. The biocompatibility of pMWNT was also studied in previous studies and the gels displayed no sign of toxicity. As demonstrated for the carbon nanotube gel hybrids, graphene is well embedded into the gel matrix and does not escape. As a result, the cells or tissue were not in direct contact with the carbon nanomaterials. Furthermore, graphene hybrid gels at 0.2 mg mL^{-1} were implanted subcutaneously, stimulated for 1 min with a DC electric field of 10 V and monitored for 48 h and 7 d in order to evaluate potential inflammation or tissue damage as a result of gel implantation and electrical stimulation. The skin around the implantation site was removed and analyzed by histology (Figure S6B, Supporting Information). No signs of inflammation or necrosis were observed in both cases (48 h and 7 d), indicating that the hybrid gels were well tolerated. One way to study the severity of adverse responses was by counting the amount of leukocytes and fibroblasts present within the tissue that was in contact with the implant.[54] In H&E-stained sections, the nuclei of leukocytes and fibroblasts appear dark purple. To clearly appreciate the skin response to the implanted gels, skin section from untreated mice was used as a comparison (Figure S6B-i, Supporting Information). The skin section of the implanted mouse showed a clear increase in the number of leukocytes or fibroblasts (dark staining cells) at 48 h after implantation and electrical stimulation (Figure S6B-ii, Supporting Information). This response however seemed transient as the number of stained cells decreased on the skin section of the implanted mouse 7 d post-surgery, suggesting that the recruited cells were part of a healing process of the inflamed tissue as observed in previous studies (Figure S6B-iii, Supporting Information).[55]

The results of this study demonstrate the in vitro and in vivo performance of a previously unreported type of electroactive scaffold for on-demand drug delivery of small molecules. The mechanism of release was based on the deswelling of macroporous graphene/PMAA hydrogel hybrids upon the application of a DC electric field. Hydrogel and hydrogel nanocomposites are widely used for the development of polymeric implants for localized controlled drug delivery systems, as they have been shown to be biocompatible and have the ability to release their cargo from their reservoir-based matrix by swelling/deswelling in response of an external stimulus.[56] Many types of physical and chemical stimuli have been applied to trigger drug release from hydrogel matrices. The physical triggers include temperature, solvent composition, and field-based stimuli such as light, sound, pressure, magnetic and electric fields.

The mechanical response of electro-responsive hydrogels upon the application of an external electric field has been employed for local drug delivery with the ultimate aim of developing efficient "on-demand" drug delivery systems.[14,57–61] In all the reported studies, constant and pulsatile releases of model drugs have been achieved upon the application of an electric field, and the advantage of electro-responsive systems over other stimuli-responsive systems relies on the fact that drug release rate and quantity can be accurately controlled by modulating the strength of the electric field. However, controlled drug delivery from such systems remains, to date, in its infancy mainly due to the problems common to all hydrogels such as slow hydrogel response to the field and low amounts of drug dose released upon electrical stimulation. An alternative to these issues encountered with hydrogel matrices is to incorporate conductive additives to the polymer matrix in order to improve the sensitivity and response to the electrical field.

Electro-conductive hydrogels that are formed of polyanilline nanoparticles (conductive electroactive polymers CEPs) dispersed in a polyvinyl pyrrolidone (PVP) hydrogel are reported for the development of electro-stimulated drug release devices and have demonstrated promising results in programmed drug release influenced by the application of an electrical voltage.[36] In this type of electro active scaffolds, the mechanism of release is based on the transport of ions by electro-migration inside the polymeric matrix in response to oxidation or reduction.[62] However, although the use of this type of matrices allowed the progress over several milestones in the development of remote controlled delivery devices, these drug release platforms are found to suffer from some major drawbacks such as poor oxidative stability of the CEPs, in particular under repeated cycling, membrane fatigue as a result of fast switching of the CEP and poor release kinetics.[63]

Several groups have used carbon nanotubes as conductive additives to enhance the electro-sensitivity hydrogel properties.[64,65] These studies reported interesting results, where the response of the carbon nanotube hydrogel hybrids to the electric field was significantly improved compared to the control hydrogel (without carbon nanotubes) and more drug molecules could be released after the first electrical stimulation. However, the magnitude of hydrogel composite response to the electric

field tends to decrease with time due to the mechanical weakness of hydrogel matrices such as structural collapse or polymer degradation. We have previously observed this phenomenon in the case of the carbon nanotube hybrid hydrogels due to the alignment of MWNTs towards the anode in response to the electrical stimulation leading to partial gel matrix destruction. The use of graphene as a conductive additive significantly improved the mechanical properties of the gels compared to carbon-nanotube-based hydrogel in terms of swelling and deswelling, allowing large deformation and volumetric changes under applied electric field.

Recent papers reported the use of GO or chemically rGO as an additive for stimuli-responsive drug delivery systems, where near infrared (NIR) was used to trigger drug release from a graphene-based thermo-responsive hydrogel matrix.[30,66] In particular, a recent study demonstrated the in vitro pulsatile release of a hydrophilic model molecule from a rGO–poly (vinyl alcohol) (PVA) upon 5 min ON/OFF electrical stimulation cycles at an electrical voltage of 15 V.[28] This study reported interesting results, however the concentration of rGO used for the hybrid gel preparation was ranging from 3.3 to 16.7 mg mL^{-1}, which is about 20 to 80 times higher than the highest concentration of GBM used in our study (0.2 mg mL^{-1}). Chemically rGO, due to the presence of many defects on the carbon backbone caused by the successive oxidation and reduction process, displays significantly reduced electrical and thermal conductivity compared to pristine graphene.[19,33] In addition, the application of high electrical voltages to hydrogel-based matrix with relatively high impedance may to generate significant temperature increases as a result of "resistive" heating. This latter issue has hardly been addressed in the literature today and is crucial for the potential clinical translation of this type of devices. Pristine graphene obtained by ball-milling contains significantly less defects than GO or rGO,[67] preserving the electrical, mechanical, and thermal properties of the graphene structure. This allows the GBM gels to be more responsive than their rGO counterparts at lower graphene concentrations, require lower electrical voltages, and display a reduced temperature increases upon application of the electrical stimulation.

3. Conclusion

The present study demonstrated the in vivo capacity of an implanted electro-responsive graphene polymer hybrid for pulsatile drug release. Previous "on demand" drug delivery systems have suffered from two major issues: a) a lack of reproducibility in drug release between the ON/OFF electrical stimulation; and b) a temperature elevation during application of the electric field due to "resistive heating." The incorporation of pristine graphene at low concentrations into the electro-sensitive hydrogel matrix improved the in vivo delivery of a model drug dose under short stimulation times at low voltage, and almost entirely eliminated the "resistive heating" from the hydrogel matrix. This previously unreported electro-responsive hydrogel system was also found to be biocompatible, with minimal tissue damage. Such delivery devices can be envisioned for personalized management of chronic illnesses that require multiple dosage regimes.

Supporting Information

Supporting Information is available from the Wiley Online Library or from the author.

Acknowledgements

The authors acknowledge the 7th RTD Framework Programme—Specific Programme Cooperation (FP7-ICT-2013-FET-F-604391) for partial sponsorship of this work under the Graphene Flagship project.

Received: January 8, 2014
Revised: March 27, 2014
Published online: May 5, 2014

[1] W. D. Rhine, D. S. T. Hsieh, R. Langer, *J. Pharm. Sci.* **1980**, *69*, 265.
[2] S. Freiberg, X. Zhu, *Int. J. Pharm.* **2004**, *282*, 1.
[3] A. J. Domb, *Mol. Med. Today* **1995**, *1*, 134.
[4] S. Kempe, K. Mader, *J. Controlled Release* **2012**, *161*, 668.
[5] D. J. Overstreet, D. Dutta, S. E. Stabenfeldt, B. L. Vernon, *J. Polym. Sci., Part B: Polym. Phys.* **2012**, *50*, 881.
[6] Y. Samchenko, Z. Ulberg, O. Korotych, *Adv. Colloid Interface Sci.* **2011**, *168*, 247.
[7] C. P. McCoy, C. Brady, J. F. Cowley, S. M. McGlinchey, N. McGoldrick, D. J. Kinnear, G. P. Andrews, D. S. Jones, *Expert Opin. Drug Delivery* **2010**, *7*, 605.
[8] B. P. Timko, T. Dvir, D. S. Kohane, *Adv. Mater.* **2010**, *22*, 4925.
[9] H. L. Liu, M. Y. Hua, H. W. Yang, C. Y. Huang, P. C. Chu, J. S. Wu, I. C. Tseng, J. J. Wang, T. C. Yen, P. Y. Chen, K. C. Wei, *Proc. Natl. Acad. Sci. U.S.A.* **2010**, *107*, 15205.
[10] T. R. Kuo, V. A. Hovhannisyan, Y. C. Chao, S. L. Chao, S. J. Chiang, S. J. Lin, C. Y. Dong, C. C. Chen, *J. Am. Chem. Soc.* **2010**, *132*, 14163.
[11] X. Y. Zeng, Q. K. Zhang, R. M. Yu, C. Z. Lu, *Adv. Mater.* **2010**, *22*, 4484.
[12] S. Ramanathan, L. H. Block, *J. Controlled Release* **2001**, *70*, 109.
[13] P. Chansai, A. Sirivat, S. Niamlang, D. Chotpattananont, K. Viravaidya-Pasuwat, *Int. J. Pharm.* **2009**, *381*, 25.
[14] K. C. Wood, N. S. Zacharia, D. J. Schmidt, S. N. Wrightman, B. J. Andaya, P. T. Hammond, *Proc. Natl. Acad. Sci. U.S.A.* **2008**, *105*, 2280.
[15] J. Ge, E. Neofytou, T. Cahill, R. Beygui, R. Zare, *ACS Nano* **2012**, *6*, 227.
[16] J. T. F. Keurentjes, M. F. Kemmere, H. Bruinewoud, M. Vertommen, S. A. Rovers, R. Hoogenboom, L. F. S. Stemkens, F. Peters, N. J. C. Tielen, D. T. A. van Asseldonk, A. F. Gabriel, E. A. Joosten, M. A. E. Marcus, *Angew. Chem. Int. Ed.* **2009**, *48*, 9867.
[17] A. Servant, L. Methven, R. P. Williams, K. Kostarelos, *Adv. Healthcare Mater.* **2013**, *2*, 803.
[18] K. S. Novoselov, V. I. Fal'ko, L. Colombo, P. R. Gellert, M. G. Schwab, K. Kim, *Nature* **2012**, *490*, 192.
[19] N. O. Weiss, H. L. Zhou, L. Liao, Y. Liu, S. Jiang, Y. Huang, X. F. Duan, *Adv. Mater.* **2012**, *24*, 5782.
[20] C. H. Lu, H. H. Yang, C. L. Zhu, X. Chen, G. N. Chen, *Angew. Chem. Int. Ed.* **2009**, *48*, 4785.
[21] H. B. Wang, Q. Zhang, X. Chu, T. T. Chen, J. Ge, R. Q. Yu, *Angew. Chem. Int. Ed.* **2011**, *50*, 7065.
[22] L. Y. Feng, Y. Chen, J. S. Ren, X. G. Qu, *Biomaterials* **2011**, *32*, 2930.
[23] O. Akhavan, E. Ghaderi, R. Rahighi, *ACS Nano* **2012**, *6*, 2904.
[24] L. Z. Feng, S. A. Zhang, Z. A. Liu, *Nanoscale* **2011**, *3*, 1252.
[25] J. T. Robinson, S. M. Tabakman, Y. Y. Liang, H. L. Wang, H. S. Casalongue, D. Vinh, H. J. Dai, *J. Am. Chem. Soc.* **2011**, *133*, 6825.

[26] Y. Wang, D. Zhang, Q. Bao, J. J. Wu, Y. Wan, *J. Mater. Chem.* **2012**, *22*, 23106.
[27] J. F. Shen, B. Yan, T. Li, Y. Long, N. Li, M. X. Ye, *Soft Matter* **2012**, *8*, 1831.
[28] H. W. Liu, S. H. Hu, Y. W. Chen, S. Y. Chen, *J. Mater. Chem.* **2012**, *22*, 17311.
[29] J. Q. Liu, C. F. Chen, C. C. He, L. Zhao, X. J. Yang, H. L. Wang, *ACS Nano* **2012**, *6*, 8194.
[30] C. W. Lo, D. F. Zhu, H. R. Jiang, *Soft Matter* **2011**, *7*, 5604.
[31] O. Akhavan, E. Ghaderi, *J. Mater. Chem. B* **2013**, *1*, 6291.
[32] O. Akhavan, E. Ghaderi, *Nanoscale* **2013**, *5*, 10316.
[33] T. S. Sreeprasad, V. Berry, *Small* **2012**, *9*, 341.
[34] X. Huang, X. Y. Qi, F. Boey, H. Zhang, *Chem. Soc. Rev.* **2012**, *41*, 666.
[35] V. Leon, M. Quintana, M. A. Herrero, J. L. G. Fierro, A. de la Hoz, M. Prato, E. Vazquez, *Chem. Commun.* **2011**, *47*, 10936.
[36] A. Guiseppi-Elie, *Biomaterials* **2010**, *31*, 2701.
[37] A. C. Ferrari, J. C. Meyer, V. Scardaci, C. Casiraghi, M. Lazzeri, F. Mauri, S. Piscanec, D. Jiang, K. S. Novoselov, S. Roth, A. K. Geim, *Phys. Rev. Lett.* **2006**, *97*, 187401.
[38] C. Casiraghi, A. Hartschuh, E. Lidorikis, H. Qian, H. Harutyunyan, T. Gokus, K. S. Novoselov, A. C. Ferrari, *Nano Lett.* **2007**, *7*, 2711.
[39] K. S. Kim, Y. Zhao, H. Jang, S. Y. Lee, J. M. Kim, K. S. Kim, J. H. Ahn, P. Kim, J. Y. Choi, B. H. Hong, *Nature* **2009**, *457*, 706.
[40] M. M. Ozmen, O. Okay, *Polymer* **2005**, *46*, 8119.
[41] M. V. Dinu, M. M. Ozmen, E. S. Dragan, O. Okay, *Polymer* **2007**, *48*, 195.
[42] N. Annabi, J. W. Nichol, X. Zhong, C. D. Ji, S. Koshy, A. Khademhosseini, F. Dehghani, *Tissue Eng. Part B: Rev.* **2010**, *16*, 371.
[43] A. Servant, C. Bussy, K. Al-Jamal, K. Kostarelos, *J. Mater. Chem. B* **2013**, *1*, 4593.
[44] R. J. Young, I. A. Kinloch, L. Gong, K. S. Novoselov, *Compos. Sci. Technol.* **2012**, *72*, 1459.
[45] D. Bitounis, H. Ali-Boucetta, B. H. Hong, D. H. Min, K. Kostarelos, *Adv. Mater.* **2013**, *25*, 2258.
[46] H. Ali-Boucetta, D. Bitounis, R. Raveendran-Nair, A. Servant, J. Van den Bossche, K. Kostarelos, *Adv. Healthcare Mater.* **2012**, *2*, 433.
[47] A. Servant, C. Bussy, R. P. Williams, K. Kostarelos, *J. Mater. Chem.* **2013**, *1*, 4593.
[48] Z. Yan, G. X. Liu, J. M. Khan, A. A. Balandin, *Nat. Commun.* **2012**, *3*, 1.
[49] O. Akhavan, E. Ghaderi, A. Akhavan, *Biomaterials* **2012**, *33*, 8017.
[50] O. Akhavan, E. Ghaderi, H. Emamy, *J. Mater. Chem.* **2012**, *22*, 20626.
[51] O. Akhavan, E. Ghaderi, H. Emamy, F. Akhavan, *Carbon* **2013**, *54*, 419.
[52] Y. B. Zhang, S. F. Ali, E. Dervishi, Y. Xu, Z. R. Li, D. Casciano, A. S. Biris, *ACS Nano* **2010**, *4*, 3181.
[53] O. Akhavan, E. Ghaderi, *ACS Nano* **2010**, *4*, 5731.
[54] E. Henderson, B. H. Lee, Z. W. Cui, R. McLemore, T. A. Brandon, B. L. Vernon, *J. Biomed. Mater. Res. Part A* **2009**, *90A*, 1186.
[55] K. C. Dee, D. A. Puleo, R. Bizios, *An Introduction to Tissue-Biomaterial Interactions*, Wiley, New Jersey **2002,** p 127.
[56] Y. Qiu, K. Park, *Adv. Drug Delivery Rev.* **2012**, *64*, 49.
[57] K. Sawahata, M. Hara, H. Yasunaga, Y. Osada, *J. Controlled Release* **1990**, *14*, 253.
[58] I. C. Kwon, Y. H. Bae, T. Okano, S. W. Kim, *J. Controlled Release* **1991**, *17*, 149.
[59] S. H. Yuk, S. J. Lee, T. Okano, B. Berner, S. W. Kim, *Int. J. Pharm.* **1991**, *77*, 221.
[60] I. C. Kwon, Y. H. Bae, S. W. Kim, *Nature* **1991**, *354*, 291.
[61] D. J. Schmidt, J. S. Moskowitz, P. T. Hammond, *Chem. Mater.* **2010**, *22*, 6416.
[62] A. G. MacDiarmid, *Angew. Chem. Int. Ed.* **2001**, *40*, 2581.
[63] I. Stassen, T. Sloboda, G. Hambitzer, *Synth. Met.* **1995**, *71*, 2243.
[64] J. S. Im, B. C. Bai, Y. S. Lee, *Biomaterials* **2010**, *31*, 1414.
[65] J. Wu, K. S. Paudel, C. Strasinger, D. Hammell, A. L. Stinchcomb, B. J. Hinds, *Proc. Natl. Acad. Sci. U.S.A.* **2010**, *107*, 11698.
[66] Y. Z. Pan, H. Q. Bao, N. G. Sahoo, T. F. Wu, L. Li, *Adv. Funct. Mater.* **2011**, *21*, 2754.
[67] M. Quintana, M. Grzelczak, K. Spyrou, B. Kooi, S. Bals, G. Van Tendeloo, P. Rudolf, M. Prato, *Chem. Commun.* **2012**, *48*, 12159.

